COMMISSION INTERNATIONALE
DES GRANDS BARRAGES

LA 78EME CONGRES
DES GRANDS BARRAGES
Hanoi-Vietnam, may 2010

STUDY ON PARAMETERS OF GREEN'S FUNCTION METHOD FOR EVALUATING EARTHQUAKE RESISTANT CAPACITY OF HYDROPOWER FACILITIES

Yutaro Mizuhashi
Advisor, Civil Planning and Design Office, Civil and Electrical Engineering Dept. : Electric Power Development Co., Ltd.

Masayuki Kashiwayanagi, *Dr.Eng.*
Advisor, Civil Planning and Design Office, Civil and Electrical Engineering Dept. : Electric Power Development Co., Ltd.

Hiroshi Kakiage
Senior Engineer, Civil Engineering Dept.: JP Design Co., Ltd.

JAPAN

Key words : Advanced Structural Engineering

1. INTRODUCTION

Hydropower facilities consist of several civil structures and their destruction by an earthquake may damage public safety. So in place of a usual pseudo-static seismic design which has been used as before, a dynamic analysis method shall be established to clarify earthquake resistant capacity of hydropower facilities including dams against a large scale earthquake. It is necessary to estimate a large scale earthquake which may occur on a hydropower facilities' site and to evaluate seismic force acting on them by the estimated earthquake.

In Japan, many researchers have studied prediction methods of strong

ground motions since 1995 South Hyogo Prefecture Earthquake, and they proposed some prediction methods. Major prediction methods are; 1) an empirical method using attenuation relation; 2) a pseudo empirical method using the Green's function; 3) a theoretical method; and 4) a hybrid method combining the pseudo empirical method and theoretical method.

A pseudo empirical method synthesizes seismic waves of large scale earthquakes by superposing seismic waves of small scale earthquakes and there are two methods to generate seismic waves of small scale earthquakes; 1) an empirical Green's function method using observed seismic waves; and 2) a stochastic Green's function method using stochastic characteristics of seismic waves.

The stochastic Green's function method synthesizes seismic waves as follows; 1) divide assumed seismic faults into small faults; 2) calculate artificial seismic waves for each small seismic fault; 3) synthesize ground motions at the site assuming the seismic waves of the said 2) as the Green's function; and 4) decide ground motions at the site considering propagation and amplification characteristics. This method requires many parameters indicating characteristics of seismic faults, and deviations of these parameters have a great influence on generation of seismic waves, which remains to be solved.

This paper studies influences of the said parameters on calculation results of strong ground motions in the following two phase process; 1) assume strong ground motions from average parameters of seismic fault characteristics; and 2) study sensitivity of significant parameters for the results of assumption considering uncertainty of parameters.

2. METHOD OF STUDY

(1) Location of seismic fault model

Seismic faults of an assumed earthquake at the case study site consist of several faults[1] as shown in Fig. 1. The reference [1] decides magnitude and a strike of the fault model according to the fault length indicated by a broken line in the figure, however, this study assumes that the seismic faults consist of two segments, the north segment expressed by "i=1," and the south "i=2" indicated by solid lines in the figure because the fault model of the reference [1] may underestimate influence of the faults. Hereinafter, a subscript, i, indicates an index of a segment.

(2) Scale of seismic fault model

The north seismic fault model, L_1, is 36 km long and the south fault

model, L_2, is 50 km long according to Fig. 1. Their width, W, is decided as follows considering thickness of seismogenic layer. Fig. 2 shows the depth of hypocenters which occurred since October 1, 1997 to August 31, 2005 around the case study site. The figure tells that the least depth is 0 km and that there is no clear limit in the depth. The reference [2] reports that the depth of hypocenters at the case study site distributes between 0 km and 27.5 km. So this paper defines the least depth of hypocenters as 0km and the largest depth as 20 km as reported in the reference [1].

There is no information on a dip of seismic faults and this paper assumes the average dip of seismic faults as 45 degrees. Therefore, the width of a seismic fault model is calculated as (20-0)x$\sqrt{}$2=28 km.

(3) Characteristics of asperities

Based on investigations around seismic faults, one asperity lies in the north and another in the south. A circular fault plane tends to overestimate the area of asperities for seismic faults of which their length is far larger than their width compared with the existing studies. This paper assumes the area of asperities, S_{ai}, from that of seismic faults, S_i, as shown in Eq. [1] according to investigation results as explained in the reference [4].

$$S_{ai} = 0.22 \cdot S_i \qquad [1]$$

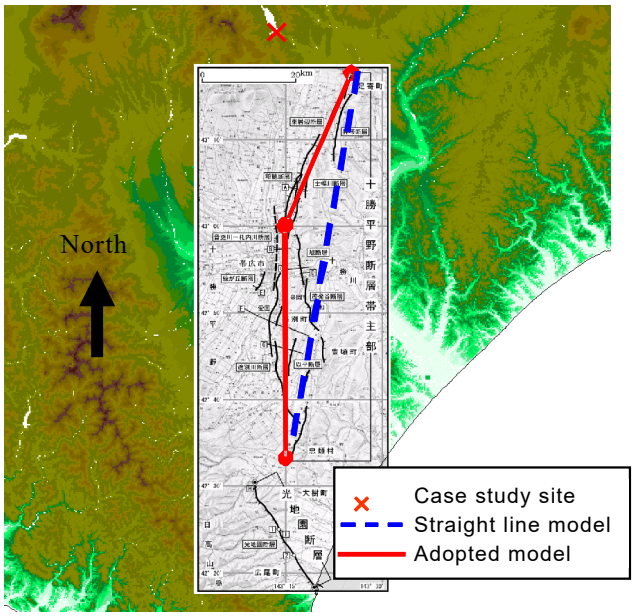

Fig. 1
Location of case study site and seismic faults
(Revise reference[1])

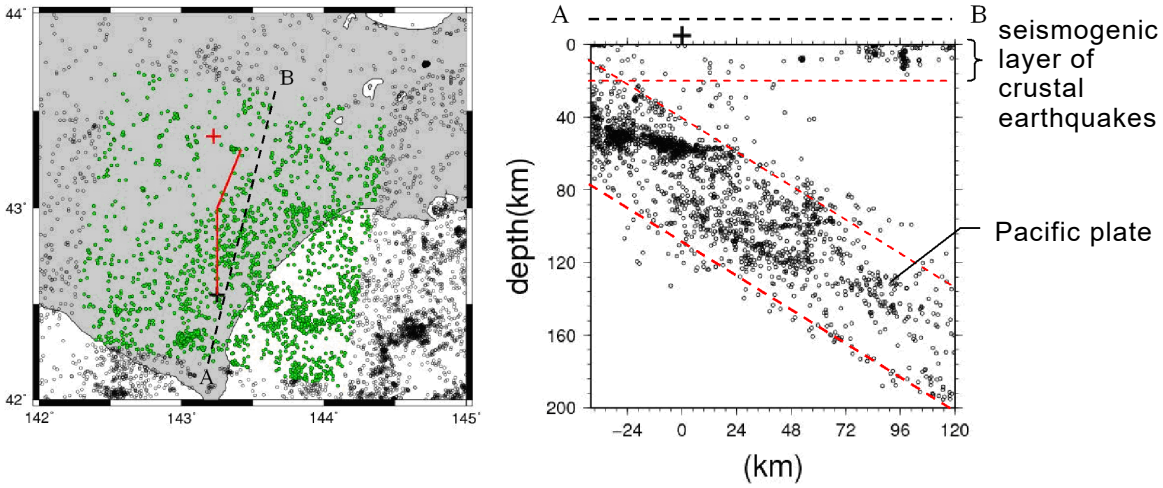

Fig. 2
Distribution of microearthquakes[3]

An average seismic slip of asperities, D_{ai}, is defined as twice the average slip of segments, D_i, as shown in Eq. [2].

$$D_{ai} = 2 \cdot D_i \qquad [2]$$

An average seismic slip in a background area, D_{bi}, is calculated by the seismic moment, M_{0bi}, and the area, S_{bi}, of the background area deducting the seismic moment of asperities, M_{0ai}, from that of segments, M_{0i}, as shown in Eq. [3] to [5].

$$M_{0ai} = \mu \cdot D_{ai} \cdot S_{ai} \qquad [3]$$

$$M_{0bi} = M_{0i} - M_{0ai} \qquad [4]$$

$$M_{0bi} = \mu \cdot D_{bi} \cdot S_{bi} \qquad [5]$$

where,
μ : Shear elastic modulus

A stress drop of asperities, $\Delta\sigma_a$, is calculated from a ratio of the area between the whole seismic faults and asperities, and an average stress drop of the whole seismic faults, $\Delta\sigma$. And an effective stress of asperities, σ_a, is assumed to be equal to its stress drop of asperities, $\Delta\sigma_a$.

$$\sigma_{ai} = \Delta\sigma_{ai} = \left(S_i / S_{ai}\right) \cdot \Delta\sigma \qquad [6]$$

This study assumes ⊿σ by Eq. [7] proposed in the reference [5] because a circular fault plane overestimates the stress drop of long seismic faults as stated above.

$$M_0 = \frac{WL}{aL+b}\Delta\sigma \qquad [7]$$

where,

M_0 : Seismic moment

W : Width of seismic fault

L : Length of seismic fault

a and b : Coefficients

The reference [5] assumes these values as follows.

a = 0.0014km^{-1}

b = 1.0

An effective stress of a background area, σ_b, is calculated by Eq. [8].

$$\sigma_{bi} = \left(D_{bi}/W_{bi}\right)/\left(D_{ai}/W_{ai}\right)\cdot\Delta\sigma_{ai} \qquad [8]$$

(4) Initial rupture point

This paper lays an initial rupture point at a south-eastern part of asperity in the southern seismic faults, R1, as shown in Fig. 3.

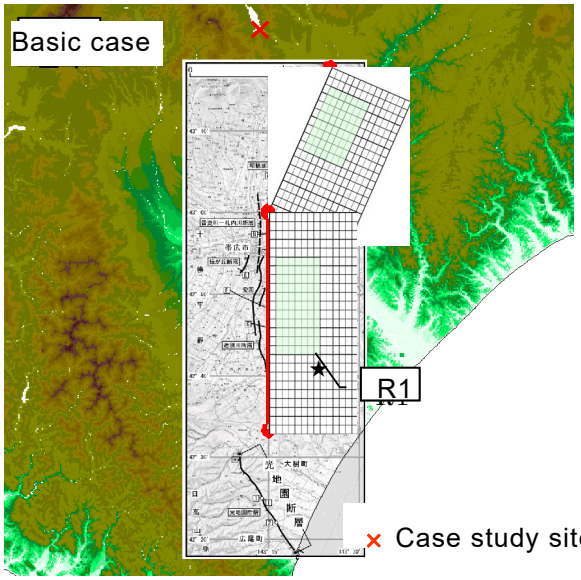

Fig. 3
Seismic fault model of basic case (revise reference[1])

(5) Parameters of hypocenter characteristics

Table 1 shows parameters used in the basic case.

Table 1
Parameters of hypocenter characteristics (Basic case)

Hypocenter characteristics			Unit	Parameter	
				North (i=1)	South (i=2)
Macroscopic characteristics	Dip		degree	45	45
	Fault length	L	km	36	50
	Fault width	W	km	28	28
	Japan Meteorological Agency magnitude	M_J		8.1	
	Total area of seismic faults	S	km^2	2,408	
	Seismic moment	M_0		3.23E+20	
	Moment magnitude	M_w		7.6	
	Secondary wave velocity	V_s	km/s	3.6	
	Average density	ρ	g/cm^3	2.8	
	Shear elastic modulus	μ	N/m^2	3.63E+10	
	Average seismic slip	D	m	3.34	3.94
	Average stress drop	Δσ	MPa	3.43	
Microscopic characteristics	Area of asperity	S_a	km^2	222	308
	Effective stress of asperity	σ_a	MPa	15.6	
Other characteristics	Initial rupture point			R1	
	Rupture propagation form			radial	
	Rupture propagation velocity	V_r	km/s	2.6	
	High-cut frequency	F_{max}	Hz	6.0	

(6) Propagation and amplification characteristics

Propagation characteristics between hypocenters and the case study site are evaluated by a Q value of the ground according to existing data. This study also assumes the ground structure at the case study site based on existing data considering its amplification effect of seismic waves which arrived from the hypocenters to the deep ground of the site. Detailed study of these characteristics is out of the scope of this study, and the reference [6] explains them instead.

2.2 STUDY ON PARAMETERS OF SEISMIC FAULTS

(1) Index for case study

This section studies sensitivity of parameters for the basic case assumed in the previous section, 2.1 considering uncertainty of parameters. An influence of variations in parameters is evaluated by spectral acceleration, peak acceleration, and a spectral intensity value, SI, calculated by Eq. [9].

$$SI = \int_{0.1}^{2.5} S_V(T,h)dT \qquad [9]$$

where,

Sv (T, h) : Velocity response spectrum
T : Period
h : Damping factor

(2) Initial rupture point (Case 1)

The basic study case laid an initial rupture point at the southern end of the southern asperity and assumed that rupture of a seismic fault would progress toward the case study site. The Case 1 lays an initial rupture point (R2, shown in Fig. 5) located at the northern part of the southern asperity so that the rupture process of two asperities may affect the case study site.

(3) High-cut frequency (Case 2)

The basic study case assumed a high-cut frequency, f_{max}, as an average value. The Case 2 assumes f_{max} as 8.3 Hz.

(4) Stress drop of asperities (Case 3)

The basic study case assumed a stress drop of asperities, $\Delta\sigma_a$, as an average value. The references [2] and [4] tell that the ratio of Eq. [6], S_i/S_{ai}, and the stress drop of asperities, $\Delta\sigma_a$, have a variation. The Case 3 assumes a stress drop of asperities corresponding to the minimum area of asperities, an area less than the average by a standard deviation, as 0.22/1.34=0.164.

(5) Arrangement of fault segments (Case 4)

The basic study case and the Cases 1 to 3 assumed two fault segments. The Case 4 assumes an asperity in a segment which passes through the center of the seismic fault zone. This case lays an asperity in the northern part and an initial rupture point at the southern end so that rupture would progress toward the case study site.

Fault length, L, of this case is shorter than that of the Cases 1 to 3 due to its shape, which results in average seismic slip, D, and stress drop, $\Delta\sigma$, small than other cases.

The stochastic Green's function method assumes the difference of a moment magnitude between small scale earthquakes and large scale ones as about 2, however, a background area is too fine for small scale seismic faults at intervals of two kilometers. So this paper assumes an interval of small scale seismic faults in a background area as 4 kilometers as shown in Fig. 4.

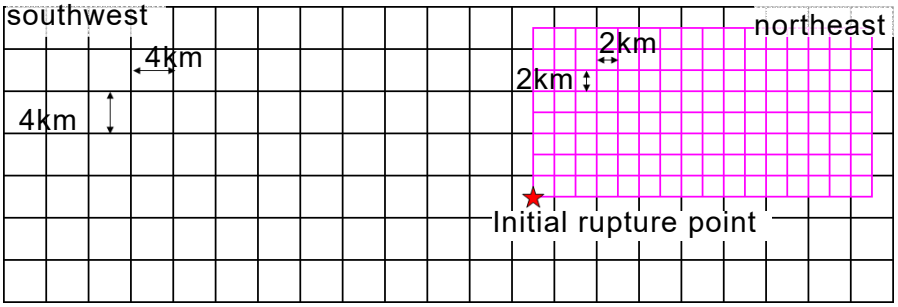

Fig. 4

Background area and small faults of asperity

(6) Summary of study case

Table 2 shows parameters of each study case and Fig. 5 shows seismic fault model of each study case.

Table 2

Parameters of hypocenter characteristics

Hypocenter characteristics		Basic case	Case 1	Case 2	Case 3	Case 4
Macroscopic characteristics	Number of segments	2				1
	Number of asperities	2				1
	Dip (degree)	45				45
	Fault length, L（km）	86（36+50）				84
	Fault width, W（km）	28				28
	Japan Meteorological Agency magnitue, M_J	8.1				8.04
	Total area of seisimic faults, S（km^2）	2,408				2,352
	Seismic moment, M_0（N-m）	3.23E+20				3.08E+20
	Moment magnitude, M_w	7.60				7.59
	Secondary wave velocity, V_s（km/s）	3.60				3.60
	Average density, ρ（g/cm^3）	2.80				2.80
	Shear elastic modulus, μ（N/m^2）	3.63E+10				3.63E+10
	Average seismic slip, D（m）	3.70				3.61
	Average stress drop, Δσ（MPa）	3.43				3.39
Microscopic characteristic	Area of asperity, S_a（km^2）	530（222+308）			395（165+230）	517
	Ratio of area of asperity to area of seismic fault（%）	22.0			16.4	22.0

Other characteristics	Effective stress of asperity, σa（MPa）	15.6			20.9	15.4
	Initial rupture point	R1 (South)	R2 (North)	R1 (South)	R1 (South)	R3
	Rupture propagation form	Radial				
	Rupture propagation velocity, V_r（km/s）	2.6				
	High-cut frequecy, F_{max}（Hz）	6.0		8.3		

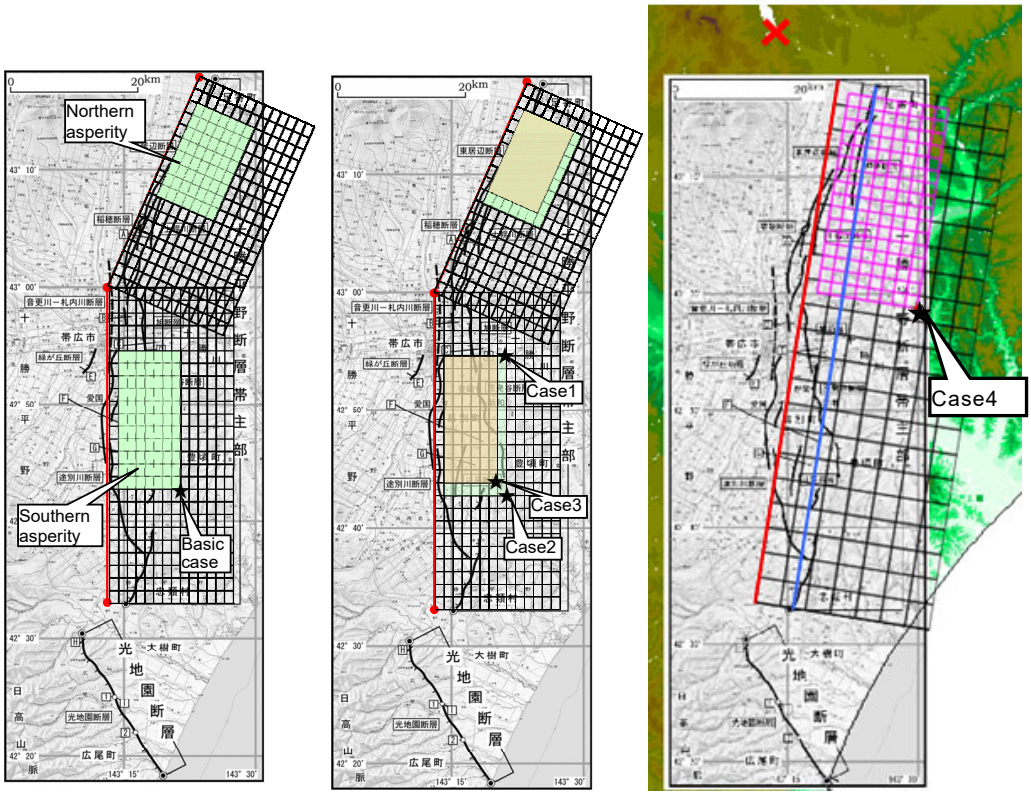

★：Initial rupture point　　×：Case study site

Fig. 5
Seismic fault model

3. STUDY RESULTS

Table 3 shows major parameters of hypocenter characteristics, and major calculation results, horizontal components in the direction of east and west of peak acceleration, SI values, and principal shock durations. Fig. 6 and Fig. 7 show spectral acceleration and acceleration time history of each study case, respectively. Generally, principal shock durations evaluated in

this study are shorter than 15 seconds, which is considered proper according to characteristics of asperities and rupture propagation velocity. The study results are considered as follows.

(1) Initial rupture point (Case 1)

The situation of rupture propagation changes as an initial rupture point is laid on the southern part of the northern asperity. Influences of each asperity fall on at the case study site. However, there is no clear difference in a spectral distribution, peak acceleration and a SI value between the basic study case and Case1, and the location of an initial rupture point assumed in this case does not amplify ground motions at the case study site.

(2) High-cut frequency (Case 2)

The Case 2 assumes a high-cut frequency as 8.3 Hz, larger than that of the basic study case, 6 Hz, and has large spectral acceleration in a shorter period, less than 0.3 second. In this case, peak acceleration is more than 20 % larger than the basic study case and a SI value is much the same. This result tells that a higher high-cut frequency assumes ground motions which are severer to hydropower facilities with shorter periods such as a dam considering that a dam has a natural period of about 0.2 second.

(3) Stress drop of asperity (Case 3)

A larger stress drop of asperities tends to amplify a short-period component of ground motions and this case gave the same results. In this case, spectral acceleration is larger than the basic study case at the period of 0.1 to 0.2 second, and peak acceleration and a SI value are larger than the basic study case, Case1 and Case2, which may give the severest ground motions to the case study site.

(4) Arrangement of fault segments (Case 4)

Spectral acceleration, peak acceleration and a SI value are larger than other cases when all seismic faults are united to one segment and asperities are concentrated at one place near the case study site. Synthetic waves have principal shock duration, related to a rupture process of asperities, half as much as other cases in which asperities are placed in a wide area, and have pulse-shaped peak acceleration.

Table 3
Major parameters of hypocenter characteristics and
major calculation results (1/2)

Hypocenter characteristics		Basic case	Case 1	Case 2	Case 3	Case 4
Macroscopic characteristics	Magnitue of earthquake	M8.1	M8.1	M8.1	M8.1	M8.04

	Number of segments	2	2	2	2	1
Microscopic characteristics	Number of asperities	2	2	2	2	1
	Stress drop	Average	Average	Average	Average -σ	Average
Other Characteristics	Initial rupture point	South	North	South	South	South
	High-cut frequecy, F_{max}（Hz）	6	6	8.3	8.3	8.3
Characteristic to basic case		Average parameter	Initial rupture point	High-cut frequency	Stress drop	Arrange-ment of seismic fault segments

Table 3
Major parameters of hypocenter characteristics and major calculation results (2/2)

		Basic case	Case 1	Case 2	Case 3	Case 4
Calcuation results	Maximum accerelation (cm/s^2)	158	150	195	186	286
	SI value (cm/s)	54	50	56	72	75
	Principal shock duration (s)	15	15	15	15	7

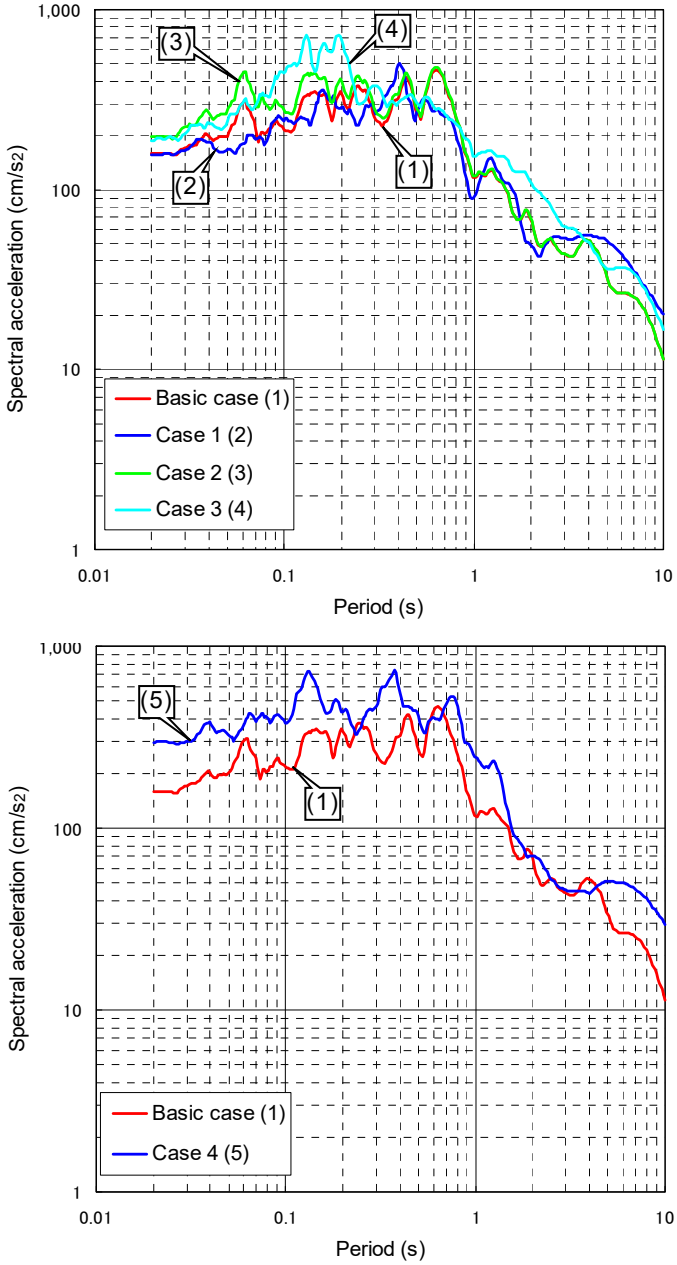

Fig. 6
Spectral acceleration of each study case
(Horizontal, EW-component)

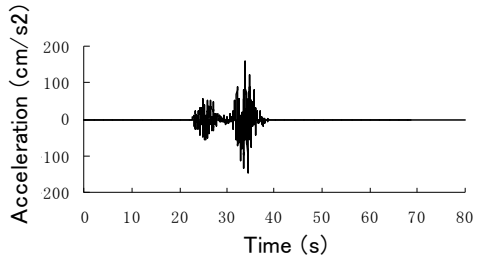

Max. 158 cm/s^2, Min 148 cm/s^2

a) Basic case

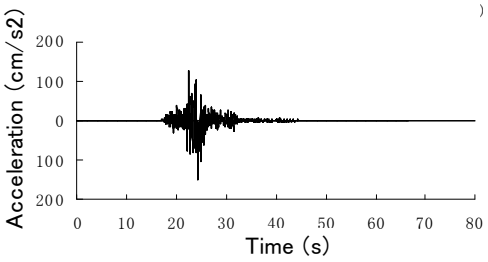

Max. 150 cm/s^2, Min 127 cm/s^2

b) Case 1

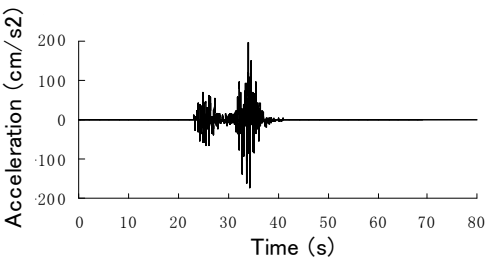

Max. 195 cm/s^2, Min 173 cm/s^2

c) Case 2

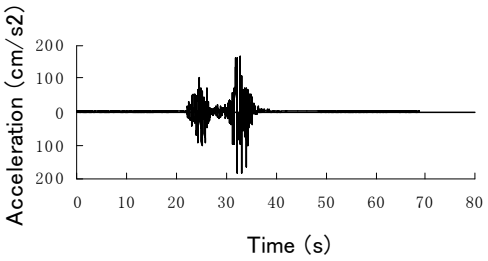

Max. 186 cm/s^2, Min 167 cm/s^2

d) Case 3

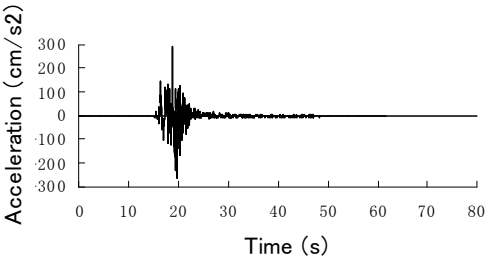

Max. 286 cm/s^2, Min 266 cm/s^2

e) Case 4

Fig.7
Acceleration time history
(Horizontal, EW-component)

4. CONCLUSION

This paper studies influences of parameters used in the stochastic Green's function method. In total, five cases were prepared by changing the following parameters; 1) area and scale of seismic faults; 2) number of

segments; 3) number and stress drop of asperities; 4) location of initial rupture point; and 5) high-cut filter characteristics.

Generally, it is considered that structures show plastic behavior under strong ground motions and that influences of strong ground motions depend on not only peak acceleration but also duration.

The study noticed that it was important to take notice of not only the maximum values of seismological characteristics but also time history and duration of seismic waves. So parameters of seismic faults shall be studied as explained in this paper in evaluating earthquake resistant capacity of hydropower facilities.

This paper extracts the study on a large scale earthquake for evaluating earthquake resistant capacity from the report “Study on earthquake resistance capacity of hydropower facilities[6]” which was conducted by the Ministry of Economy, Trade and Industry in Japan to study a quantitative method and process to evaluate soundness and an extent of damage which would occur in hydropower facilities under the influence of a large scale earthquake.

REFERENCES

[1] Long term evaluation of seismic faults in Tokachi plains. *The Headquarters for Earthquake Research Promotion*, April 13, 2005.

[2] Report on maintenance of earthquake database “SANDEL” and evaluation of maximum and minimum depth of seismogenic layer. *Japan Nuclear Energy Safety Organization*. August, 2004.

[3] *Seismological Bulletin* (CD-ROM version). Japan Meteorological Business Support Center.

[4] Kojiro Irikura, Hiroe Miyake. Prediction of Strong Ground Motions for Scenario Earthquakes. *Journal of Geography*, No. 110(6), pp.849-875, 2001.

[5] Kazuo Dan, Takayoshi Muto, Jun’ichi Miyakoshi, Motofumi Watanabe. Estimation of Effective Stress on Asperities in Inland Earthquakes Caused by Large Strike-Slip Faults and its Application to Strong Motion Simulation. *Journal of structural and construction engineering.* Transactions of Architectural Institute of Japan, No. 589, pp.81-88, March, 2005.

[6] Study on earthquake resistance capacity of hydropower facilities. *Report in fiscal 2008*. *Nuclear and Industrial Safety Agency*, Ministry of Economy, Trade and Industry, Electric Power Civil

Engineering Association, Electric Power Development Co., Ltd., Central Research Institute of Electric Power Industry. March, 2009